






REPORT



An *in vitro* FcRn- dependent transcytosis assay as a screening tool for predictive assessment of nonspecific clearance of antibody therapeutics in humans

Shan Chung ^a, Van Nguyen^a, Yuwen Linda Lin ^a, Julien Lafrance-Vanasse ^b, Suzie J. Scales ^c, Kevin Lin^d, Rong Deng^e, Kathi Williams^a, Gizette Sperinde^a, Juan Jenny Li^f, Kai Zheng^g, Siddharth Sukumaran^h, Devin Tesariⁱ, James A. Ernst^b, Saloumeh Fischer^a, Greg A. Lazar^j, Saillea Prabhu^h, and An Song ^{a*}

^aDepartment of BioAnalytical Sciences, Genentech Inc., South San Francisco, CA, USA; ^bDepartment of Protein Chemistry, Genentech Inc., South San Francisco, CA, USA; ^cDepartment of Molecular Biology, Genentech Inc., South San Francisco, CA, USA; ^dDepartment of Analytical Operations, Genentech Inc., South San Francisco, CA, USA; ^eDepartment of Clinical Pharmacology, Genentech Inc., South San Francisco, CA, USA; ^fDepartment of Biochemistry and Cellular Pharmacology, Genentech Inc., South San Francisco, CA, USA; ^gDepartment of Late Stage Pharmaceutical Development, Genentech Inc., South San Francisco, CA, USA; ^hDepartment of Pharmacokinetics & Pharmacodynamics, Genentech Inc., South San Francisco, CA, USA; ⁱDepartment of Drug Delivery, Genentech Inc., South San Francisco, CA, USA; ^jDepartment of Antibody Engineering, Genentech Inc., South San Francisco, CA, USA

ABSTRACT

A cell-based assay employing Madin–Darby canine kidney cells stably expressing human neonatal Fc receptor (FcRn) heavy chain and β 2-microglobulin genes was developed to measure transcytosis of monoclonal antibodies (mAbs) under conditions relevant to the FcRn-mediated immunoglobulin G (IgG) salvage pathway. The FcRn-dependent transcytosis assay is modeled to reflect combined effects of nonspecific interactions between mAbs and cells, cellular uptake via pinocytosis, pH-dependent interactions with FcRn, and dynamics of intracellular trafficking and sorting mechanisms. Evaluation of 53 mAbs, including 30 marketed mAb drugs, revealed a notable correlation between the transcytosis readouts and clearance in humans. FcRn was required to promote efficient transcytosis of mAbs and contributed directly to the observed correlation. Furthermore, the transcytosis assay correctly predicted rank order of clearance of glycosylation and Fv charge variants of Fc-containing proteins. These results strongly support the utility of this assay as a cost-effective and animal-sparing screening tool for evaluation of mAb-based drug candidates during lead selection, optimization, and process development for desired pharmacokinetic properties.

ARTICLE HISTORY

Received 20 October 2018
Revised 22 February 2019
Accepted 8 March 2019

KEYWORDS

Cell-based assay; FcRn; monoclonal antibody; pharmacokinetics; transcytosis



Introduction

Therapeutic monoclonal antibodies (mAbs) have become a major class of pharmaceutical products due to their proven effectiveness in the treatment of a variety of diseases. Whereas many conventional mAbs exhibit pharmacological behavior similar to those of the endogenous IgGs, substantial heterogeneity in nonspecific clearance of mAb drugs in human is commonly observed. Slow clearance from circulation enables desired drug concentrations to be realized with lower doses or infrequent dosing, which reduces the cost of care and improves patient compliance. Therefore, proper evaluation and selection of candidate drugs for desirable pharmacokinetic (PK) properties is imperative to successful development of mAb-based biotherapeutics.^{1,2}


Nonspecific clearance is a key PK parameter of mAbs that reflects the antibody's target-independent elimination from circulation. It occurs mostly through intracellular catabolism after cellular uptake by pinocytosis in the reticuloendothelial system. Nonspecific clearance of mAbs can be influenced by a number of biophysical, biochemical, and biological properties. These include isoelectric point (pI),³ charge,^{4,5} hydrophobicity,⁶ nonspecific

binding,⁷ off-target binding,⁸ glycosylation pattern,^{9,10} binding affinity toward Fc γ receptors,¹¹ immunogenicity,¹² and interactions with neonatal Fc receptor (FcRn)^{13–15} which plays a key role in serum IgG homeostasis. FcRn is well recognized for its role in salvaging internalized IgGs from degradation to extend their half-lives in circulation.^{16,17} Internalized molecules that are not bound to FcRn are directed to lysosomes for degradation. While the contribution of FcRn in prolonging half-lives of Fc-containing proteins is well documented, binding to FcRn is not the sole determinant for PK behavior of Fc-containing proteins, as evidenced by reports of a lack of correlation between FcRn binding and clearance of mAbs *in vivo*.^{7,14}

FcRn is a heterodimeric protein consisting of a transmembrane major histocompatibility complex class-I like heavy chain and a soluble light chain, β 2 microglobulin (B2M). FcRn binds to the Fc domain of IgGs at acidic pH (pH <6.5), but only minimally at neutral or basic pH (pH \geq 7.0). This pH-dependent binding property allows FcRn to bind to internalized IgGs in acidic endosomes and transport them back to the cell surface, where they are released into the circulation at physiological pH (pH \sim 7.4). This FcRn-mediated recycling pathway is

CONTACT Shan Chung  chung.shan@gene.com  Department of BioAnalytical Sciences, Genentech Inc., South San Francisco, CA, USA

*Present address: Immune-Onc Therapeutics, 4030 Fabian Way, Palo Alto, CA 94303

 Supplemental data for this article can be accessed on the [publisher's website](#).

© 2019 The Author(s). Published with license by Taylor & Francis Group, LLC.

This is an Open Access article distributed under the terms of the Creative Commons Attribution-NonCommercial-NoDerivatives License (<http://creativecommons.org/licenses/by-nc-nd/4.0/>), which permits non-commercial re-use, distribution, and reproduction in any medium, provided the original work is properly cited, and is not altered, transformed, or built upon in any way.

generally considered to be instrumental to extension of IgG half-life and maintenance of their levels in circulation. In addition to the recycling pathway, FcRn also mediates transcytosis of IgGs from vascular space out into tissue compartment, which impacts PK of mAbs by affecting their distribution. FcRn-mediated transcytosis is most well known for its role in the intestinal absorption of maternal IgG in neonatal rodents and the transplacental transport of maternal IgG in humans.¹⁶⁻¹⁸ In this function, FcRn binds to IgGs either in endosomes or at the cell surface (for cells that are bathed at acidic pH such as intestinal epithelial cells), guides them to the opposite side of the cell surface and then releases them to various destinations, including interstitial space. This FcRn-mediated transcytosis pathway is bidirectional and is inherently polarized depending on physiological needs to direct the majority of its IgG cargo either away from or toward the circulation.^{19,20} Since both recycling and transcytosis direct internalized mAbs away from lysosomes, both pathways contribute to the IgG salvage function of FcRn by regulating catabolism of mAbs, and are expected to affect mAbs' nonspecific clearance *in vivo*.

Studies in animals^{21,22} and nonhuman primates²³ have been routinely conducted to predict PK of mAbs in humans. However, these studies are time consuming and costly, and often involve animal sacrifice. Furthermore, translation of PK results from animal studies to humans is not straightforward, in part due to species differences in FcRn binding, target-dependent drug disposition, and induction of anti-drug immune responses.²⁴ On the other hand, a wide variety of *in vitro* assays have been developed to predict *in vivo* PK behavior of mAbs. These assays were typically designed to assess specific physicochemical properties of mAbs that are known to affect PK behavior, such as nonspecific binding,⁷ binding to extra-cellular matrix (ECM),²⁵ or interactions with FcRn.^{26,27} However, due to the multiplicity of factors involved in clearance, none of these assays has shown consistent success in predicting PK of mAbs. Given the nature of FcRn as an intracellular trafficking molecule, the dynamics of endosomal sorting and trafficking of Fc-containing molecules are expected to affect the efficiency of the FcRn-mediated salvage mechanism, and hence the nonspecific clearance of mAbs. In addition, the processes of cellular uptake via pinocytosis or endocytosis could also play a role in determining the rate and extent of IgG catabolism. Engineered cell lines expressing stably transfected FcRn have been used to study the structure and function of FcRn, as well as FcRn-mediated intracellular trafficking pathways.²⁸⁻³⁰ Cell-based assays employing such cell lines are promising tools for predictive assessment of PK properties of antibody-based drug candidates.

Transcytosis assays using Madin–Darby canine kidney (MDCK) cells stably expressing human FcRn have been developed to support development of engineered antibodies or antibody domains with enhanced FcRn binding and engineered FcRn-binding peptide fusion proteins.³¹⁻³³ The transcytosis readouts from these assays appeared to correlate with test molecules' *in vivo* clearance. Similar assays have been used to characterize FcRn binding of therapeutic antibodies and Fc-fusion proteins, including wild-type (WT) and engineered Fc variants with varying FcRn binding affinities, as well as oxidized and aggregated antibody samples.³⁴ Further, a human endothelial cell-based recycling assay was developed

to support preclinical screening of Fc-engineered human IgG1 variants and showed correlations between recycling efficiency and half-lives in human FcRn transgenic mice.³⁵ However, none of these assays have demonstrated consistently the capability to predict PK behavior of conventional IgGs carrying regular Fc sequences.

Here, we describe the development and characterization of an FcRn-dependent cell-based assay that measures transcytosis of regular mAbs in MDCK cells expressing human FcRn under conditions resembling the FcRn-mediated IgG salvage pathway. The output of this assay is attributable to not only Fc-FcRn interactions at physiological conditions, but also nonspecific binding, cellular uptake, sorting, and intracellular trafficking processes pertaining to *in vivo* PK behavior of mAbs. Based on the evaluation of 53 mAbs with diverse structure, function, and pharmacological properties, we found a notable correlation between transcytosis outputs and clearance of mAbs in humans. To our knowledge, this is the first reported correlation between an *in vitro* readout and an *in vivo* PK parameter for a large group of conventional human/humanized antibodies. This novel *in vitro* assay offers an unprecedented utility to biopharmaceutical scientists as a time-efficient, cost-effective, and animal-sparing tool for evaluation of mAb-based drug candidates during lead selection and optimization, and process development for desired PK properties.

Results

Development of an FcRn-mediated transcytosis assay

The MDCK cell line was co-transfected with human FcRn heavy chain (FCGRT) and B2M genes. Cells expressing both genes were isolated by flow cytometry. A clonal cell line (MDCK-hFcRn; 305-6) expressing high levels of FCGRT and B2M on cell surface (Figure 1) was selected for development of an FcRn-dependent transcytosis assay. Expression of the transfected human FcRn was characterized by immunofluorescence microscopy using antibodies recognizing FCGRT, transferrin receptor (a recycling endosome marker), and LAMP1 (a late endosome and lysosome marker). Consistent with a published report,³⁶ the human FcRn in MDCK-hFcRn cells was expressed mostly in intracellular compartments and co-localized with transferrin receptor but not LAMP1 (Figure 2).

For the transcytosis assay, cells were grown to confluence on filter membranes in trans-well plates. Test molecules were added to the growth medium in the inner chamber and allowed to incubate for 24 h. Test molecules transported through the cells were released into the medium in the outer chamber and quantified by enzyme-linked immunosorbent assay (ELISA). The assay was optimized for seeding density, trans-well plate format, loading concentration, assay medium, and assay duration (data not shown). Of note, since the assay medium contained fetal bovine serum (FBS), the human FcRn is expected to engage test antibodies while binding to bovine albumin.³⁷ Therefore, the setup of the assay allows assessment of FcRn-mediated intracellular trafficking of test antibodies under relevant physiological conditions.

The assay was qualified to demonstrate suitable precision and specificity. The precision of the assay was determined by

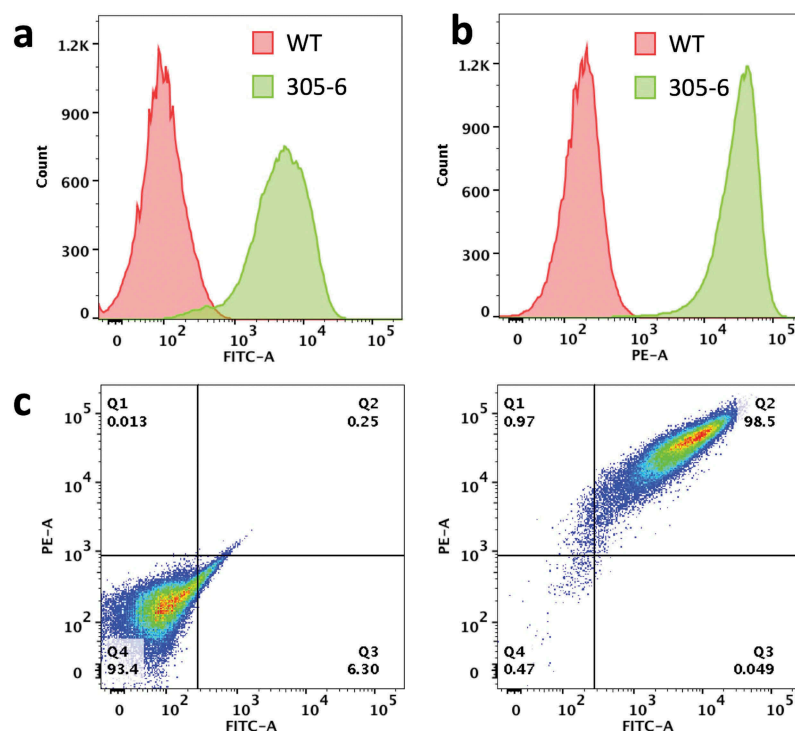


Figure 1. Expression of human FcRn heavy chain and B2M in the clonal MDCK cell line (MDCK-hFcRn; 305-6). (a) Flow cytometry histogram of cell surface expression of B2M in WT and 305-6 cells. (b) Flow cytometry histogram of cell surface expression of FCGR2B in WT and 305-6 cells. (c) Flow cytometry data represented as a dot plot: cell surface expression of FCGR2B (y-axis) and B2M (x-axis) in WT (left panel) and 305-6 (right panel) cells.

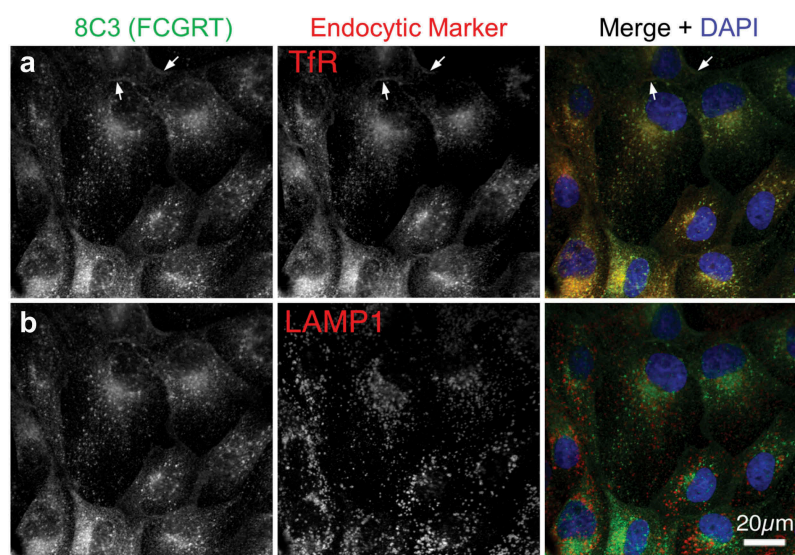


Figure 2. Intracellular localization of transfected human FcRn in MDCK cells. MDCK-hFcRn cells were fixed and triple stained for FcRn heavy chain (FCGRT, green) and either the recycling endosome marker transferrin receptor (TfR, a) or the late endosomal and lysosomal marker LAMP1 (b). Both endocytic markers are shown in red in the merges with nuclear DAPI (blue) so that any colocalization, appearing as yellow, can be readily compared. Arrows indicate plasma membrane signals.

calculating overall variability of transcytosis values of the bevacizumab reference material from six independent runs. The mean transcytosis value is 3.5 ng/mL with a standard deviation value of 0.36. The average intra-assay precision is 7.7% and overall inter-assay precision is 9.5%. The specificity of the assay was demonstrated by testing molecules either without Fc (ranibizumab, an anti-vascular endothelial growth factor A antigen-binding fragment [Fab]) or carrying Fc with mutations that abolish FcRn binding (anti-herpes simplex

virus glycoprotein D [gD]-HAHQ antibody). The transcytosis values of ranibizumab and the anti-gD-HAHQ antibody were 0.3 and 0.8 ng/mL, significantly lower than those of bevacizumab and anti-gD WT antibody at 3.5 and 3.0 ng/mL, respectively. Results of this study demonstrate the specificity of the assay for molecules carrying function Fc fragments. In addition, effects of antibody concentration on transcytosis were evaluated by testing bevacizumab at a starting concentration of 3000 μg/mL, followed by threefold serial dilutions.

Increasing the loading concentration of bevacizumab in our assay clearly led to more effective transcytosis in a concentration-dependent manner (Supplementary Figure S1).

Correlation of *in vitro* transcytosis output with *in vivo* clearance of mAbs in humans

A panel of 53 mAbs, including 30 marketed therapeutic antibodies and 23 clinical mAb candidates, were tested in the assay and the transcytosis outputs were analyzed for potential correlations with their clearance in humans. The mAbs chosen for this study were based on the availability of clinical-grade materials and documented human PK data. These mAbs are highly diversified in terms of IgG subclass, target property (soluble vs. membrane-bound), mechanism of action (blocking/antagonistic vs. depletion), and route of administration. Several molecules contain engineered mutations that alter their effector functions (e.g., atezolizumab and durvalumab), enable association of bi-specific half antibodies (e.g., emicizumab), or stabilize IgG4 Fab arms (e.g., nivolumab and pembrolizumab). However, none of the test molecules contain mutations that were designed to modulate their PK or FcRn interactions. In addition to the transcytosis assay, most molecules were also evaluated for nonspecific binding activity by the baculovirus (BV) ELISA⁷ or FcRn binding affinity at pH 6.0 with a biolayer interferometry-based method.²⁷ The assay results, the clearance in humans, and selective biochemical/biological properties of the mAbs are presented in Table 1. The mean transcytosis output of the mAb panel is 5.4 ng/mL with a median of 4.7 and a range of 2.6–14.9, which reflects an average of about 0.005% of the materials loaded in the inner chamber (100 µg/mL). The respective mean, median, and range of FcRn binding affinity at pH 6.0 was 0.6, 0.54, and 0.25–1.8 µM and 0.25, 0.06, and 0.04–3.9 for BV ELISA score. The human clearance values of 30 marketed mAb drugs were obtained from the drug's prescribing information or published reports, and those of the 23 clinical stage mAbs were generated from clinical studies conducted at Genentech. The mean, median, and range of clearance in human are 5.0, 4.1, and 1.4–14.1 mL/d/kg. The wide ranges of assay results and clearance values further indicate the substantial diversity of the mAbs tested in this study.

As shown in Figure 3(a), an apparent trend of association was observed between the transcytosis outputs and clearance of the mAbs ($R^2 > 0.8$). It appeared that antibodies with faster clearance in humans showed higher transcytosis outputs in the assay. Of note, the observed correlation was not affected by sub-grouping test molecules based on marketed or development molecules, target property (membrane-bound or soluble), or route of administration (intravenous vs. subcutaneous injection; Supplementary Figure S2). On the other hand, clearance showed no apparent correlation with FcRn binding affinity (Figure 3(b)) or BV ELISA score that reflects nonspecific binding (Figure 3(c)). Of note, additional transcytosis experiments were performed using selective test molecules and a different clonal MDCK-hFcRn cell line 305-2 that expressed about 50% lower level of human FcRn than 305-6. It appeared that both cell lines supported the transcytosis assay and showed similar trends of correlation between the transcytosis outputs of the test

molecules and their respective clearance in humans (Supplementary Figure S3). Therefore, this finding was likely attributable to expression of human FcRn in MDCK cells, and not due to unique properties of a specific human FcRn-transfected MDCK cell line.

To demonstrate the dependence of FcRn in both the transcytosis output and the observed correlation with clearance, ten mAbs from the panel were tested in the same assay using the untransfected MDCK cells. As expected, transcytosis outputs from the untransfected MDCK cells were in general less than 20% of those from the MDCK-hFcRn cells (Table 2), and showed no apparent correlation with clearance in humans (Figure 4(a)). On the other hand, transcytosis in MDCK-hFcRn cells with the same set of mAbs shows a strong correlation with clearance (Figure 4(b)). These results support that expression of FcRn is required to promote efficient transcytosis of test molecules in this assay and contributes directly to their observed correlation with clearance in humans. However, given the complexity of this cell-based transcytosis assay, it is not surprising that FcRn binding alone showed no correlation with transcytosis (Table 2). In fact, whereas antibodies engineered for enhanced FcRn binding have shown extended half-lives *in vivo*, lack of correlations between FcRn binding and PK properties of both regular and engineered mAbs have been well documented.^{7,14,37} Therefore, the lack of correlation between transcytosis and FcRn binding is actually consistent with current understating of molecular mechanisms underlying PK of mAbs that FcRn interaction is a required function, but not the sole determinant for their clearance *in vivo*.

Impact of cell binding on transcytosis of mAbs

Transcytosis of test molecules in our assay required binding and internalization by MDCK-hFcRn cells. Test molecules may bind to the cells via nonspecific interactions or specific binding to surface molecules at physiological pH, both of which may affect transcytosis output. To evaluate the effect of cell binding on transcytosis, ten mAbs were incubated with MDCK-hFcRn and MDCK cells, and the levels of bound antibodies were assessed by flow cytometry. No significant difference was observed in binding activity between the two cell lines, indicating minimal binding by the mAbs to human FcRn at physiological pH (Table 2). Further, no apparent correlation between cell binding and the transcytosis output or clearance with either cell lines was observed (Supplementary Figures S4(A–D)). However, elevated binding to both cell lines was observed with trastuzumab and pertuzumab (Table 2). Since human epidermal growth factor receptor 2 (HER2) shares 92% amino acid homology with its canine counterpart,⁴² the observed binding of anti-HER2 antibodies to MDCK cells is likely due to cross-reactivity to canine epidermal growth factor receptor-2 (EGFR-2). In fact, the canine EGFR-2 contains both HER2 interaction sites recognized by trastuzumab and pertuzumab, each contains one single amino acid change, histidine 296 to asparagine for pertuzumab,⁴³ and proline 557 to serine for trastuzumab.⁴⁴ It appeared that the moderate increase in binding to MDCK cells by trastuzumab did not result in increased transcytosis in untransfected MDCK cells, and that its transcytosis value in the MDCK-hFcRn cells remained consistent with its clearance in humans. On the other

Table 1. Summary of biochemical and pharmacological properties of test antibodies including their clearance values in humans, and results from the transcytosis assay, FcRn binding assay, and BV ELISA.

No.	Test antibody	Subclass	Clearance in humans (mL/d/kg)	Transcytosis (ng/mL)	FcRn Binding	BV ELISA	Target	ROA
					pH 6.0 K _D (μM)			
1	Trastuzumab	IgG1/Kappa	2.9 ^a	2.7	0.68	0.038	M	IV
2	Omalizumab	IgG1/Kappa	2.4 ^b	2.7	0.37	0.041	S	SC
3	Rituximab	IgG1/Kappa	4.8	5.6	0.46	0.103	M	IV
4	Ocrelizumab	IgG1/Kappa	2.4	4.8	0.45	0.045	M	IV
5	Pertuzumab	IgG1/Kappa	3.4	6.8	0.57	0.047	M	IV
6	Bevacizumab	IgG1/Kappa	3.1	3.4	0.56	0.150	S	IV
7	Atezolizumab	IgG1/Kappa	2.9	3.0	0.65	0.050	M	IV
8	Tocilizumab	IgG1/Kappa	4.3	5.5	0.46	0.049	M	SC
9	Efalizumab	IgG1/Kappa	7.3 ^c	8.3	1.80	0.091	M	SC
10	Obinutuzumab	IgG1/Kappa	1.4	4.5	0.49	0.046	M	IV
11	Emicizumab	IgG1/Kappa	3.4	3.6	1.23	0.050	S	SC
12	Ofatumumab	IgG1Kappa	3.2	4.3	0.55	0.059	M	IV
13	Vedolizumab	IgG1/Kappa	2.2	4.1	0.61	0.071	M	IV
14	Adalimumab	IgG1/Kappa	4.1	4.7	1.18	0.058	S	SC
15	Natalizumab	IgG4/Kappa	5.5	4.9	0.28	0.037	M	IV
16	Nivolumab	IgG4/Kappa	2.8	4.3	0.25	0.053	M	IV
17	Pembrolizumab	IgG4/Kappa	2.8	4.2	0.29	0.085	M	IV
18	Avelumab	IgG1/Lambda	8.4	7.3	1.30	0.155	M	IV
19	Cetuximab	IgG1/Kappa	8.1	6.1	0.34	0.039	M	IV
20	Palivizumab	IgG1/Kappa	2.8	3.8	0.48	0.075	S	IM
21	Infliximab	IgG1/Kappa	4.5 ^d	5.6	0.80	2.683	S	IV
22	Olaratumab	IgG1/Kappa	8.0	8.2	0.38	0.049	M	IV
23	Panitumumab	IgG2/Kappa	4.9	5.0	0.78	0.037	M	IV
24	Reslizumab	IgG4/Kappa	2.4	3.3	0.45	0.088	S	IV
25	Basiliximab	IgG1/Kappa	14.1	14.9	0.54	0.234	M	IV
26	Ixekizumab	IgG4/Kappa	5.1	5.1	ND	0.061	S	SC
27	Durvalumab	IgG1/Kappa	2.8	6.0	0.70	0.058	M	IV
28	Evolocumab	IgG2/Kappa	4.1	3.6	ND	ND	S	SC
29	Alirocumab	IgG1/Kappa	11.4	9.9	ND	ND	S	SC
30	Golimimumab	IgG1/Kappa	7.5	6.8	ND	ND	S	SC
31	mAb1	IgG1/Kappa	3.5	4.5	1.29	0.066	M	SC
32	mAb2	IgG4/Kappa	2.8	4.0	0.95	0.053	S	IV
33	mAb3	IgG1/Lambda	4.4	3.1	0.40	0.207	M	IV
34	mAb4	IgG1/Kappa	6.3	8.2	0.26	0.046	M	IV
35	mAb5	IgG1/Kappa	2.0	3.3	0.37	0.051	M	SC
36	mAb6	IgG1/Kappa	8.5	7.4	ND	0.480	M	IV
37	mAb7	IgG1/Kappa	9.5	7.1	0.94	0.045	S	SC
38	mAb8	IgG1/Kappa	5.8	6.9	ND	0.341	M	SC
39	mAb9	IgG1/Kappa	3.2	3.9	0.61	0.146	S	IV
40	mAb10	IgG1/Kappa	5.3	5.0	0.40	3.916	M	IV
41	mAb11	IgG4/Kappa	2.2	2.6	0.65	0.038	S	SC
42	mAb12	IgG1/Lambda	10.6	10.2	ND	1.745	S	SC
43	mAb13	IgG1/Kappa	4.3	3.9	0.42	0.042	M	IV
44	mAb14	IgG2/Kappa	2.4	4.0	0.70	0.075	M	SC
45	mAb15	IgG1/Kappa	4.0	4.4	0.38	0.045	M	IV
46	mAb16	IgG1/Kappa	2.9	3.6	1.24	0.134	S	SC
47	mAb17	IgG1/Kappa	4.5	3.8	0.73	0.296	M	IV
48	mAb18	IgG1/Lambda	2.7	3.9	0.44	0.041	S	IV
49	mAb19	IgG1/Kappa	3.0	5.1	0.48	0.048	S	IV
50	mAb20	IgG1/Kappa	2.7	4.0	0.40	0.051	S	SC
51	mAb21	IgG1/Kappa	10.3	8.4	ND	0.071	M	IV
52	mAb22	IgG1/Kappa	13.8	10.6	0.41	0.147	M	IV
53	mAb23	IgG1/Kappa	7.2	6.2	0.75	0.044	S	SC
Mean			5.0	5.4	0.63	0.25		
SD			3.0	2.4	0.33	0.69		
Median			4.1	4.7	0.54	0.06		
Range			1.4–14.1	2.6–14.9	0.25–1.8	0.038–3.916		

Data are shown as averages of reportable values from at least two independent experiments. With the exception of those specified, clearance values were obtained from the US Food and Drug Administration-approved prescribing information or generated from clinical studies sponsored by Genentech.

ND = not done; ROA = route of administration; M = membrane-bound; S = soluble; SC = subcutaneous injection; IV = intravenous injection; IM = intramuscular injection.

^aQuartino *et al.* 2016.³⁸

^bQuartino *et al.* 2017.³⁹

^cNg *et al.* 2005.⁴⁰

^dKlotz *et al.* 2007.⁴¹

hand, a substantial increase in binding to MDCK cells was observed for pertuzumab, which showed noticeably higher transcytosis in both cell lines, but similar clearance in humans, compared to trastuzumab. It is likely that the increased transcytosis by pertuzumab was an assay artifact due to its increased

binding to canine EGFR-2 and enhanced internalization/uptake via receptor-mediated endocytosis. The lower binding to MDCK cells (compared to trastuzumab) and minimum impact on transcytosis by trastuzumab could be due to the proline 557 to serine substitution in canine EGFR-2, which may lead to reduced

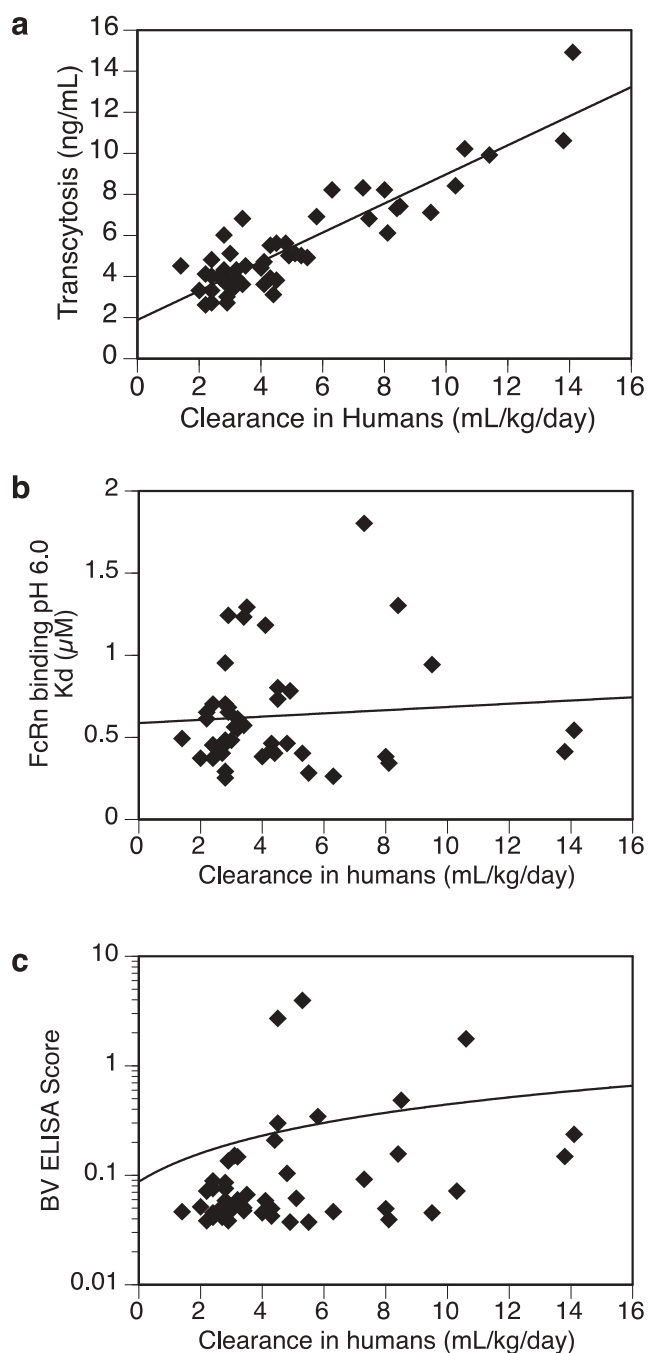


Figure 3. Relationships between test antibodies' clearance in humans and (a) transcytosis outputs in MDCK-hFcRn cells, (b) FcRn binding affinity at pH 6.0, (c) non-specific binding activity by BV ELISA. Total number of antibodies tested: (a) = 53, (b) = 45, (c) = 50.

binding with trastuzumab and possibly compromised cellular uptake.

Impact of charge on transcytosis of mAbs

Antibodies with high pIs or more positive Fv charge have been shown to exhibit faster clearance than their lower pI/less positively charged counterparts,^{3,4} likely due to their enhanced electrostatic interaction with the cells or ECM.⁴⁵ To evaluate the effect of charge on transcytosis, two sets of

Table 2. Cell surface binding and transcytosis of test antibodies in MDCK cells and MDCK-FcRn cells.

Test antibody	Transcytosis in MDCK cells (ng/mL)	Transcytosis in MDCK-hFcRn cells (ng/mL)	Clearance in humans (mL/d/kg)	Binding to MDCK cells (MFI)	Binding to MDCK-hFcRn cells (MFI)
Bevacizumab	0.3	3.4	3.1	81	102
Trastuzumab	0.3	2.7	2.9	178	336
Pertuzumab	1.1	6.8	3.4	1005	1354
Ocrelizumab	0.5	4.8	2.4	78	101
Basiliximab	1.1	14.8	14.1	111	203
Infliximab	0.7	5.6	4.5	99	128
Adalimumab	0.5	4.7	4.1	77	183
Reslizumab	0.6	3.3	2.4	74	93
mAb6	0.3	7.4	8.5	111	168
mAb12	0.5	10.2	10.6	103	233
No mAb	NA	NA	NA	75	94

Transcytosis data are shown as averages of reportable values from at least two independent experiments. Cell binding activity was determined by flow cytometry. MFI = mean fluorescence intensity.

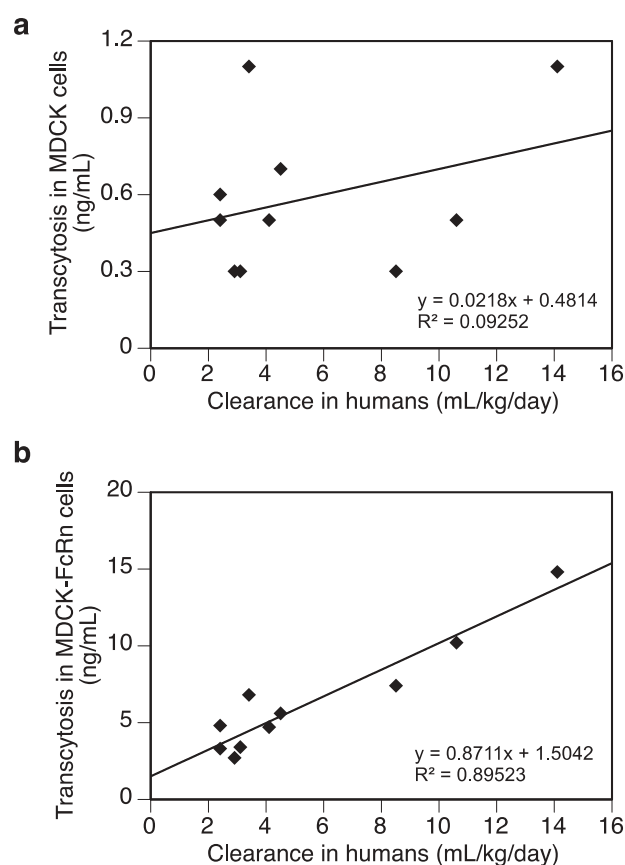


Figure 4. (a) A lack of correlation between transcytosis outputs of test antibodies in the untransfected MDCK cells and their clearance in humans. (b) Correlation between transcytosis outputs of test antibodies (same as those in Figure 4(a)) in MDCK-hFcRn cells and their clearance in humans. Data were fitted with a linear regression model and both the equation and the R -squared value are presented. Total number of antibodies tested = 10.

charge variants based on two humanized IgG1 mAbs, anti-lymphotoxin α (anti-LT α), or humAb4D5-8 (anti-HER2) were tested. Each set of samples included the parent molecule, one that had a more positively charged Fv and one that had a less positively charged Fv. With the exception of the less positively charged anti-HER2-4, the effect of Fv charge on PK behaviors

of these molecules in cynomolgus monkeys was demonstrated in a previous study.⁴ Consistent with the observed correlation between transcytosis and clearance, the more positively charged variants (anti-LT α +3 and anti-HER2+5) showed higher transcytosis and faster clearance, whereas the less positively charged variant (anti-LT α -4) showed lower transcytosis and slower clearance (Table 3). Therefore, the transcytosis output correctly predicted the observed rank order of clearance of the charge variants and demonstrated that our assay is capable of assessing effects of charge on clearance of mAbs *in vivo*. On the other hand, the less positively charged anti-HER2-4 showed slightly higher transcytosis and faster clearance. While we do not fully understand the root cause for this discrepancy, it is possible that the engineered mutations in anti-HER2-4 might have inadvertently altered other biochemical properties of the molecules, resulting into neutralized effects. Nevertheless, the fact that the transcytosis output of this molecule correctly matched its clearance and not the charge further supports our hypothesis that the output of the transcytosis assay may be attributable to most of the major factors known to affect PK, but reflects only combined effects of these factors.

The impact of electrostatic interactions on transcytosis and clearance was further examined. The combined Fv ($V_L + V_H$) charge and pI values of 20 mAbs were determined (Supplementary Table S1) and their relationships with the transcytosis outputs or clearance in humans were analyzed. As shown in Figure 5(a,b), no apparent trend of association was observed between clearance and either combined Fv charge or pI ($R^2 < 0.25$). On the other hand, the correlation between clearance and transcytosis remains strong ($R^2 > 0.8$) with this subset of mAbs (Figure 5(c)).

Impact of glycosylation on transcytosis of Fc-containing molecules

Glycosylation patterns of mAbs or Fc-fusion proteins can significantly affect their PK and pharmacodynamics behaviors.^{9,10,46} To determine the effects of glycosylation on transcytosis, two sets of Fc-containing molecules were tested. The first set included a humanized IgG1 mAb, ocrelizumab (2H7-WT), and its deglycosylated (2H7-DG), afucosylated (2H7-AF), and mannose-5 (2H7-Man5) glycoform variants. The second set was based on X-Fc, a fusion protein consisting of a human glycoprotein X and human IgG1 Fc. Three variants of X-Fc with high, medium, and low level of sialylation

Table 3. Transcytosis and clearance of test antibodies with varying Fv charges.

mAb ID	Clearance in cynomolgus monkey ^a (mL/d/kg)	Transcytosis in MDCK-hFcRn cells (ng/mL)	Fv charge ^a
Anti-LT α -4	5.78	3.8	4.1
Anti-LT α	14.9	6.0	8.1
Anti-LT α +3	59.3	16.0	11.1
Anti-HER2-4	6.63	3.2	2.1
Anti-HER2	6.22	2.7	6.1
Anti-HER2+5	51.1	20.5	11.1

^aFrom Bumbaca Yadav, D. *et al.*⁴

Transcytosis data are shown as averages of reportable values from at least two independent experiments.

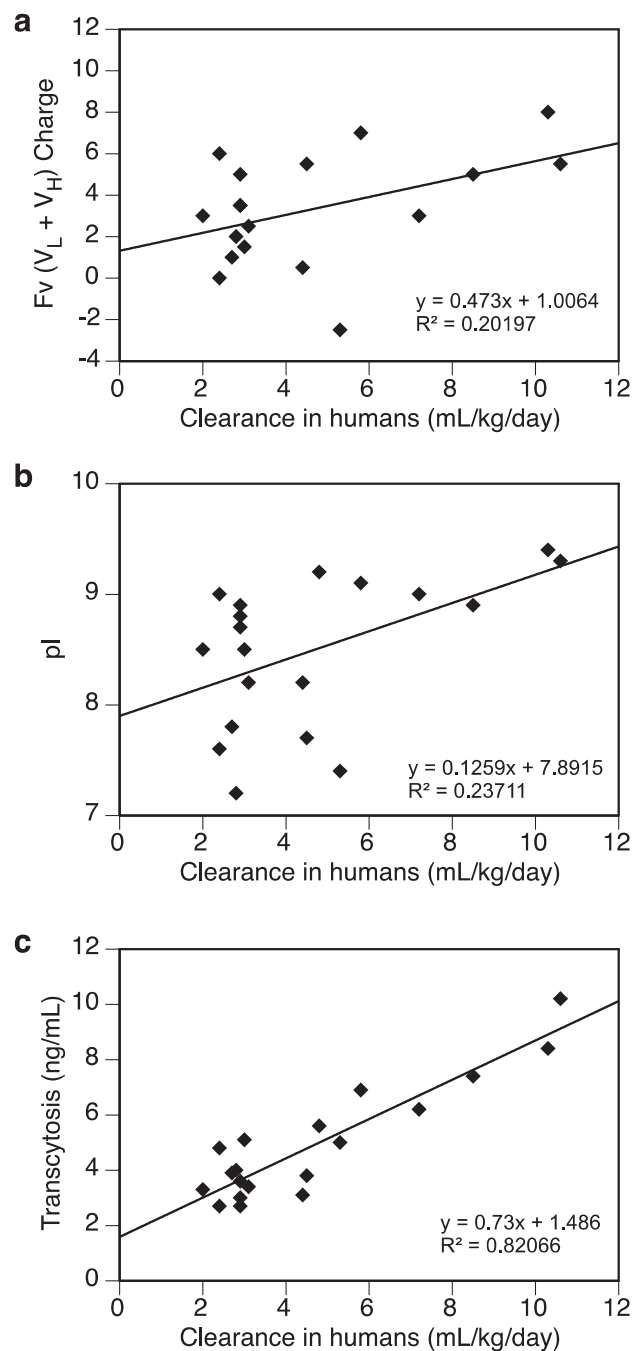


Figure 5. Relationships between test antibodies' clearance in humans and their (a) Fv ($V_L + V_H$) charge, (b) pI, (c) transcytosis output. Data were fitted with a linear regression model and both the equation and the R -squared value are presented. Fv charge was calculated at pH 5.5 and pI was measured by imaged capillary isoelectric focusing. Total number of antibodies tested = 20.

(X-Fc-SA-H, X-Fc-SA-M, and X-Fc-SA-L, respectively) were tested. The clearance values of 2H7-WT and 2H7-Man5 in mice were obtained from a published study;¹⁰ the clearance values of the X-Fc sialylation variants were generated from a mouse study described in the "Materials and methods" section. While no clearance data were available for 2H7-DG and 2H7-AF, mAbs depleted of Fc N-glycans or core-fucose have been shown to exhibit similar PK compared to WT antibodies.⁴⁷ As shown in Table 4, compared to the 2H7-WT, similar transcytosis outputs were observed for 2H7-DG

Table 4. Summary of pharmacokinetics parameters, cell binding, and transcytosis outputs of test antibodies with varying N-glycans or FcRn binding activities.

Test antibody	Description	Clearance in mice (mL/d/kg)	Half-life in cynomolgus monkey (d)	Transcytosis in MDCK-hFcRn cells (ng/mL)	Cell binding to MDCK-hFcRn cells (MFI)
2H7	Humanized IgG1 mAb	9.89 ^a	NA	4.8	140
2H7-AF	Afucosylated	NA	NA	4.1	163
2H7-DG	Deglycosylated	NA	NA	4.3	160
2H7-Man5	Man-5 glycoform	27.1 ^a	NA	10.3	188
X-Fc-SA-L	Low-level sialylation Fc-fusion protein	952.5	NA	10.7	160
X-Fc-SA-M	Medium-level sialylation	132.5	NA	6	166
X-Fc-SA-H	High-level sialylation	25.1	NA	3.8	215
Anti-gD-WT	Wild-type humanized IgG1 mAb	NA	NA	3.0	347
Anti-gD-HAHQ	Reduced FcRn binding	NA	NA	0.8	161
Anti-gD-YTE	Enhanced FcRn binding	NA	NA	7.0	1153
Anti-VEGF	Wild-type humanized IgG1 mAb	NA	11.4 ^b	3.4	ND
Anti-VEGF-QA	Enhanced FcRn binding	NA	24.9 ^b	5.1	ND

Transcytosis data are shown as averages of reportable values from at least two independent experiments. Cell binding activity was determined by flow cytometry.

NA = not available; MFI = mean fluorescence intensity.

^aYu *et al.* 2012.¹⁰

^bYeung *et al.* 2010.³⁷

and 2H7-AF, whereas twofold increase was observed for 2H7-Man5. Therefore, clearances of 2H7-DG and 2H7-AF were predicted to be similar to 2H7-WT, whereas 2H7-Man5 was predicted to exhibit faster clearance, both of which were confirmed by their expected/observed relative clearance values in mice. On the other hand, the three X-Fc sialylation variants showed decreasing levels of transcytosis in an order consistent with decreased amount of terminal galactose as a result of increased sialylation. The predicted rank order for clearance of these sialylation variants is consistent with the observed clearance data from the mouse study (Table 4).

Binding of the mannose receptor⁴⁸ and the asialoglycoprotein receptor⁴⁹ on cell surface by high-mannose and sialylated glycoproteins has been implicated as the cause for their accelerated clearance. We performed cell binding study to investigate this possibility, but did not observe any notable differences in binding to MDCK-hFcRn cells among the two sets of glycosylation variants (Table 4). This suggests that the increase in transcytosis was likely not due to binding to specific receptors on MDCK cells. However, further studies are needed to confirm the presence or absence of such receptors on MDCK cells.

Impact of altered FcRn binding on transcytosis

Antibodies engineered for enhanced FcRn binding have been shown to exhibit slower clearance and prolonged half-lives.^{13,14,37} To investigate transcytosis behavior of mAbs with altered FcRn binding affinity, two sets of humanized IgG1 mAbs were tested. One set included an anti-vascular endothelial growth factor WT antibody (anti-VEGF-WT) and an anti-VEGF-QA antibody with T307Q/N434A mutations that increase FcRn binding up to tenfold.³⁷ The other set included an anti-gD-WT antibody, and two of its FcRn binding variants, anti-gD-HAHQ with H310A/H435Q mutations that reduce FcRn binding to undetectable levels,⁵⁰ and anti-gD-YTE with M252Y/S254T/T256E mutations that increase FcRn binding for more than tenfold.¹³

As shown in Table 4, all five molecules showed detectable transcytosis with anti-gD-HAHQ showing the lowest output likely due to its inability to bind to FcRn. However, contrary to results from the mAb panel where increased transcytosis output correlated with increased clearance, both the anti-VEGF-QA and the anti-gD-YTE antibodies that exhibit slow clearance *in vivo* showed increased transcytosis compared to their WT counterparts (Table 4). Cell binding studies revealed that the anti-gD-YTE antibody bound to MDCK-hFcRn cell at a significantly higher level compared with the WT version (Table 4), likely due to its enhanced binding to FcRn at neutral pH. These findings indicate that molecules exhibiting altered binding affinity for FcRn via protein engineering may behave differently than mAbs carrying typical Fc in this assay.

Discussion

Using MDCK cells stably expressing human FcRn, we developed a cell-based assay that measures transcytosis efficiency of mAb under conditions relevant to the FcRn-mediated IgG salvage pathway. This assay provides an ideal model system for predictive assessment of clearance of mAbs in humans by assessing the combined effects of nonspecific binding to cells, cellular uptake via pinocytosis, pH-dependent interactions with FcRn, and dynamics of intracellular trafficking, and sorting processes. Evaluation of 53 mAbs with diverse structure, function, and pharmacological properties in this assay revealed a notable correlation between the transcytosis outputs and clearance in humans. The transcytosis output also correctly predicted the impact of glycosylation and charge variations on clearance. It is worth noting that the observed correlation between the transcytosis readout and clearance in humans may apply to a broad range of mAbs carrying typical Fc regions, but not to those engineered for substantially altered FcRn or FcγR binding activities. Additionally, caution should be taken in cases where the test antibodies exhibit

unusual binding to MDCK cells due to cross-reactivity to canine cell-surface proteins.

The expression of human FcRn appeared to be required for efficient transcytosis in the assay, and contributed directly to the observed correlation between the transcytosis readout and clearance in humans. In the absence of FcRn, the untransfected MDCK cells mediate very low levels of transcytosis that showed no correlation with clearance. However, consistent with published reports that FcRn binding affinity (at acidic pH) does not in general predict PK behavior of mAbs,^{7,14,37} FcRn binding affinity also does not correlate with *in vitro* transcytosis efficiency. Nevertheless, FcRn binding analysis for mAbs tested in this study showed that molecules with the same Fc sequences may exhibit vastly different FcRn binding affinities at pH 6.0 (up to sevenfold differences among mAbs carrying IgG1 heavy chain and kappa light chain), which is consistent with previous reports that additional molecular attributes of the Fab region may impact overall FcRn interaction of the mAb.⁵¹

Nonspecific binding to cells affects both the rate of internalization and off-target retention that may contribute to a faster clearance *in vivo* and more efficient transcytosis in our assay. Nonspecific interactions due to electrostatic attractions between cationized molecules and anionic heparan sulfate proteoglycans have been implicated in cellular internalization of macromolecules.⁴⁵ The BV ELISA that detects binding to BV particles is a useful tool for evaluation of nonspecific binding of therapeutic proteins.⁷ In this study, the BV ELISA scores of 49 mAbs showed no apparent correlation with human clearance. Further, of the 12 mAbs with the top 25% of scores, only half of them exhibit fast clearance in humans (>6 mL/kg/d). In addition, evaluation of Fv charge, pI, and binding activity to both untransfected MDCK and MDCK-hFcRn cells also failed to reveal any notable correlations with either transcytosis or clearance. It appears that neither FcRn binding affinity nor nonspecific binding parameters can be used alone to predict the test molecules' transcytosis output or clearance due to multiplicity of factors involved in these functions.

Glycosylation is also known to influence the distribution and catabolism of mAbs *in vivo*. It has been reported that liver cells expressing asialoglycoprotein receptors bind to galactose residues in glycoproteins without terminal sialylation and mediate their endocytosis and eventual degradation/clearance.^{49,52} In addition, Kupffer and sinusoidal endothelial cells in liver, as well as macrophages and dendritic cells in blood and tissue, express mannose-binding receptors that bind and clear mAbs carrying high-mannose glycans.⁵³ It is unknown if MDCK cells express asialoglycoprotein receptors or mannose-binding receptors; however, our results showed no distinct pattern of differential binding to untransfected MDCK and MDCK-FcRn cells among the glycoform variants tested. It is possible that the presence of glycans with terminal mannose or sialic acid provides additional properties that influence the output of the neutral pH transcytosis assay that happens to correlate with their impact on PK. For example, sialylation results in an increase in the net negative charge of mAbs and lowers their pI value, thereby leading to formation of acidic variants that bind favorably to the anionic

component of mammalian cell membranes. While we did not observe any notable increase in binding to MDCK cells, it is possible that the increase in net charge due to the addition of sialic acid might affect intracellular trafficking parameters, which in turn affected the output of the transcytosis assay. In any case, the results of this study suggest the involvement of additional mechanisms in the clearance of high-mannose and highly sialylated glycoform variants in humans.

A number of cell-based assays employing MDCK cells transfected with human FcRn have been developed to support development of therapeutic proteins with prolonged half-lives in humans.³¹⁻³⁵ While some of these assays showed notable correlations between assay output and clearance of engineered molecules with enhanced FcRn binding, none were able to predict clearance of conventional mAbs. In these assays, test molecules were typically loaded into the inner chamber of transwells with acidic buffer (pH <6.0) and the transcytosed molecules were harvested in the outer chamber with basic buffer (pH >7.4). The assay was designed to take advantage of the pH-dependent binding characteristic of FcRn to facilitate the cellular uptake of test molecules via binding with the FcRn on cell surface under acidic conditions and the release of the test molecules under basic conditions. However, these assays are inherently flawed for predictive assessment of PK behavior of mAbs. Since the transfected cells express high levels of FcRn and the assay is performed under acidic conditions, the test antibodies exhibiting high binding affinity toward FcRn will readily bind to FcRn and enter the cells via FcRn-mediated endocytosis. This is in contrast to what happens *in vivo*, where antibodies bind minimally to FcRn at physiologic pH, and cellular uptake is mainly mediated by nonspecific fluid-phase pinocytosis. Since the outputs of these transcytosis assays are heavily influenced by the antibody's FcRn-binding affinity at acidic pH, they cannot properly reflect the contribution of other factors known to impact PK, such as nonspecific binding, electrostatic interactions, and intracellular trafficking parameters. In addition, incubation of the cells under acidic conditions limits the duration of the assay and may potentially create additional assay artifacts. It is possible that the attempts to use these assays to predict clearance of conventional mAbs *in vivo* have not been successful because of these limitations.

FcRn-mediated recycling and transcytosis pathways share several functional characteristics: both are mediated by FcRn, both divert the FcRn complexed IgG away from lysosome, and both involve intracellular trafficking through cells.¹⁸ We initially assumed that both pathways contribute to protection of IgG from lysosomal degradation and hypothesized that an increase in transcytosis reflects an increase in recycling, which translates to more efficient rescue of the internalized IgG, and hence reduced degradation by lysosome and reduced clearance. This hypothesis was supported by the behavior of mAbs with Fc mutations that significantly alter their FcRn binding affinity. Consistent with their extended half-life and reduced clearance, both mAbs with higher FcRn binding affinity (anti-VEGF-QA and anti-gD-YTE) showed increased transcytosis compared to their low FcRn binding counterparts. However, the results of the mAb panel showed an opposite trend of correlation, where mAbs with faster clearance were

transcytosed more efficiently. This discrepancy may be explained by increased binding to FcRn in neutral pH that enhance cellular uptake of the mAbs in this assay. Alternatively, the substantially enhanced FcRn binding may affect interactions with the sorting mechanisms and dynamics between the recycling and transcytosis pathways. It has been reported that the extent of recycling vs. transcytosis may vary depending on the cell type and the availability of adaptor proteins.¹⁸ For example, in the lactating mammary gland where both recycling and transcytosis of IgG appears to occur, IgG molecules with high affinity for FcRn were delivered less efficiently into the milk than those IgG molecules of lower affinity.⁵⁴

Whereas the recycling pathway is responsible for transporting internalized IgG back to circulation, the transcytosis pathway transports IgG between vascular space and tissue compartment for specific physiological needs, e.g., the transplacental transport of maternal IgG to fetus.⁵⁵ The fact that IgG is present in secretions of various mucosal sites supports that FcRn function *in vivo* to transport IgGs across various cell barriers for immune surveillance and host defense.^{16,56} The observed correlation between transcytosis and clearance suggests that FcRn-mediated transcytosis may inadvertently serve as an elimination mechanism of antibodies pertaining to their PK.

Given the complexity of *in vivo* mechanisms involving absorption, distribution, metabolism, and elimination of antibodies, it is unlikely that any single *in vitro* system can consistently and accurately predict PK behavior of mAb drugs in humans. Nevertheless, by incorporating human FcRn in a cell-based assay with an intracellular trafficking readout relevant to the FcRn-mediated IgG salvage pathway, the transcytosis assay described here is well equipped to provide an output that reflects the target-independent, nonspecific clearance mechanism of mAbs in humans. Whereas the assay appears to be applicable to a diverse group of Fc-containing molecules and responds to factors known to impact PK, it remains to be determined if the correlation observed in this report represents a fortuitous coincidence or a revelation that may fundamentally change our views on FcRn-mediated transcytosis pertaining to PK of mAb drugs.

This report demonstrates for the first time a correlation between an *in vitro* readout and *in vivo* PK parameter of mAbs. Despite the discussed limitations and need for further mechanistic investigations, this cell-based assay offers drug developers an unprecedented tool for *in vitro* evaluation of potential liabilities in nonspecific clearance of drug candidates to support lead selection and optimization, with the aim to rank order candidates and reduce the number of molecules tested in animal models. In addition, the addition/inclusion of the transcytosis data may facilitate development of improved mechanism-based PK models to support design of optimal dose and dosing schemes in clinical studies.

Materials and methods

Test molecules

The test molecules included a panel of 53 mAbs with documented clearance values in humans, 3 Fc-fusion proteins and additional 12 mAbs (4 charge variants, 3 glycosylation

variants, and 5 FcRn binding variants). In the mAb panel, 30 are marketed therapeutic antibodies of which 19 (ofatumumab, vedolizumab, adalimumab, natalizumab, nivolumab, pembrolizumab, avelumab, cetuximab, palivizumab, infliximab, olaratumab, panitumumab, reslizumab, basiliximab, ixekizumab, durvalumab, evolocumab, alirocumab, golimumab) were purchased from the manufacturers. The remaining antibodies were produced in engineered Chinese hamster ovary (CHO) cells at Genentech (South San Francisco, CA, USA).

The deglycosylated ocrelizumab was produced by incubating 1 mg of ocrelizumab with 275 units of PNGase F (Cat# P0705, New England Biolabs, Ipswich, MA, USA) at 37°C for 24 h and further purified through a protein A column. The Man-5 glycoform of ocrelizumab was produced by addition of kifunensine (Cat# 1000943, Cayman Chemical Company, Ann Arbor, MI, USA) to the cell culture media at 5 mg/L as an α -mannosidase inhibitor to prevent removal of extra mannose molecules in the endogenous glycosylation pathway. The Man8/9 glycoforms obtained from the cell culture process with kifunensine addition were purified through a protein A column. The purified glycoforms at 10 mg/mL were then incubated with 20 mU/mL α -mannosidase I (Cat# GKX-5009, ProZyme, Hayward, CA, USA) at 37°C for 24 h to produce Man5 glycoforms *in vitro*.

The sialylated Fc fusion proteins, X-Fc-SA-L, X-Fc-SA-M, and X-Fc-SA-H, were produced and purified from an engineered CHO cell line at Genentech.

Production and characterization of charge variants of anti-LT α and humAb4D5-8 (anti-HER2) were as previously described.⁴ Production of FcRn-binding variants of anti-gD and anti-VEGF was as previously described.^{37,57}

Generation and characterization of MDCK cells expressing human FcRn

MDCK II cells (European Collection of Authenticated Cell Cultures, Salisbury, UK) were grown in Dulbecco's modified minimal essential media (DMEM) containing 10% FBS (Clontech, Mountain View, CA, USA), 100 units/mL penicillin, 100 μ g/mL streptomycin, and 0.292 mg/mL L-glutamine (Cat# 10378016, Thermo Fisher Scientific, Waltham, MA, USA) in a 37°C, 5% CO₂ humidified incubator. Cells were transfected by electroporation with a modified pRK plasmid containing cDNA for human FCGRT (UniProtKB-P55899, FCGRTN_HUMAN) and B2M (UniProtKB - P61769, B2MG_HUMAN) separated by a P2A sequence⁵⁸ and under control of a cytomegalovirus promoter. After 3 d, the cells were selected with 5 μ g/mL of puromycin and expanded for 2 weeks.

Cells were then sorted for FCGRT expression by fluorescence-activated cell sorting (FACS) using an anti-FCGRT antibody (Cat# ADM31, Aldevron, Fargo, ND, USA) and a secondary anti-mouse phycoerythrin (PE)-conjugated antibody (Cat# A10543, Thermo Fisher Scientific). All clones were maintained with constant selection agent (5 μ g/mL puromycin). The final clone was chosen based on both FCGRT and B2M cell surface expression assessed by flow cytometry using anti-human B2M fluorescein isothiocyanate (FITC)-conjugated antibody

(Cat# 2M2, BioLegend, San Diego, CA, USA) as described below.

The MDCK-II cells were grown to confluence and detached using a non-enzymatic cell dissociation reagent (Cat# C5914, Sigma Aldrich, St. Louis, MO, USA). Cells were first stained with an anti-FCGRT antibody in PBS, 0.05 M ethylenediaminetetraacetic acid (EDTA), 2% bovine serum albumin (BSA) for 1 h on ice. After washing, the cells were incubated with an anti-mouse PE-conjugated secondary antibody and with an anti-B2M FITC-conjugated antibody for 1 h on ice, in the dark. The samples were washed and resuspended in PBS, 0.05M EDTA, 2% BSA for flow cytometry analysis on a BD FACSCanto II (BD Biosciences, San Jose, CA, USA). A clonal cell line (MDCK-hFcRn 305-6) expressing high levels of FCGRT and B2M on cell surface (Figure 1) was selected for further development of the FcRn-dependent transcytosis assay.

To characterize expression of transfected FcRn in MDCK cells, hFcRn-MDCK-II cells were plated at 5000 cells/well on 8-well LabTek-II slides for 4 d, fixed at 85% confluency in 3% paraformaldehyde (Electron Microscopy Sciences, Hatfield, PA, USA) for 20 min at room temperature and quenched for 10 min with 50 mM NH₄Cl. Saponin buffer (0.4% saponin, 1% BSA, 2% FBS in PBS) was used for subsequent permeabilization, blocking, antibody incubations, and wash steps. Primary antibodies were 1 µg/ml 8C3 anti-FCGRT (mouse IgG2b, Genentech), 1 µg/ml rabbit anti-LAMP1 (Cat# 24170, Abcam, Burlingame, CA, USA) and 0.5 µg/ml anti-transferrin receptor (H68.4, mouse IgG1, Cat# 13-6890, Invitrogen, Carlsbad, CA, USA), applied for 1 h at room temperature. Respective secondary antibodies were Alexa 488 anti-mouse IgG2b (Cat# A21141, Invitrogen), Alexa 647 anti-mouse IgG1 (Invitrogen A21240), and Cy3 anti-rabbit (Cat# 711-166-152, Jackson ImmunoResearch Laboratories). Coverslips were mounted using Prolong Gold with DAPI (Cat# P36931, Invitrogen). Slides were imaged on a spinning disk confocal (Zeiss 3i W AxioObserver M1) with a 63× PlanAPO N.A. 1.4 objective controlled by SlideBook (v6) with 405, 488, 561, and 640 nm lasers and detected with a Hamamatsu FLASH 4.0 sCMOS camera. Figures were assembled in Photoshop CS5.1, with gamma levels adjusted across the whole image for brightness.

Transcytosis assay

Cells were seeded at a density of 1×10^5 cells/well in cell growth medium (DMEM High Glucose supplemented with 10% FBS, 100 units penicillin/streptomycin, and 5 µg/mL puromycin) in 96-well trans-well plates (Cat# CLS3381, Corning Costar, Corning, NY, USA), with 100 and 200 µL of medium in the inner and outer chambers, respectively. Cells were used for experiments on the second day post-plating. The medium in the inner chamber was removed and test molecules were added to a final concentration of 100 µg/mL (0.67 µM) and incubated for 24 h at 37°C. The functional integrity of filter-grown MDCK-hFcRn cells was monitored by measuring trans-epithelial electrical resistance (TEER). The TEER of monolayers before the assay typically ranged from 250 to 300 Ω·cm², a characteristic range for polarized MDCK II cells.³⁰ The barrier integrity (leakiness) of the monolayer during the assay was monitored by spiking Lucifer Yellow (Lucifer Yellow CH, dilithium salt; Cat# L0259, Sigma Aldrich) along with the test molecules in the inner

chamber. Lucifer Yellow prepared in cell growth medium was added in the final 90 min of the 24-h assay incubation. Media from the outer chamber were collected and the amount of transcytosed molecules was determined by ELISA. The level of passive passage of Lucifer Yellow during the assay was calculated by dividing the florescent signal in samples from the outer chamber by that of the inner chamber. Transcytosis results from wells exhibiting greater than 0.1% of passive passage of Lucifer Yellow in the outer chamber were discarded.

The output of the assay represents the concentration (ng/mL) of the transcytosed molecule in the medium of outer chamber and the reportable value of the assay is average concentration of three replicate wells from the same plate.

Quantification of transcytosis

The concentration of transcytosed molecules in the medium of an outer chamber was measured with a sandwich ELISA as described in Chung *et al.*³⁴ Briefly, a 96-well microtiter plate was coated with goat anti-human IgG-F(ab)' (Cat# 109-006-088, Jackson ImmunoResearch Laboratories, West Grove, PA, USA) in a sodium carbonate buffer (pH 9.6) at 2–8°C overnight. After washing with PBS, 0.05% polysorbate-20 and blocking with PBS, 0.5% BSA, 0.1% casein, 0.05% P20, 0.05% Proclin300, serially diluted assay standards, controls, or samples in assay diluent (PBS, 0.5% BSA, 0.05% P20, 0.05% Proclin300) were added to the plate. After incubation and washing, the plate was incubated with goat anti-human IgG-Fc conjugated to horseradish peroxidase (HRP; Cat# 109-035-008, Jackson ImmunoResearch Laboratories) in assay diluent followed by addition of 3,3',5,5'-tetramethylbenzidine (TMB) solution (Cat# 50-76-00, Kirkegaard & Perry Laboratories, Gaithersburg, MD, USA). Color was allowed to develop for 15 min without agitation, and the reaction was stopped by the addition of 1 M H₃PO₄. The absorbance was read at 450 nm with a 650 nm reference wavelength on a Spectra Max I3 plate reader (Molecular Devices Corporation, Sunnyvale, CA, USA). The data were processed using the SoftmaxPro software provided by the manufacturer. Concentrations of test antibodies in samples were interpolated from on a standard curve fitted with a four-parameter logistic model generated from the same plate.

For Fc-fusion proteins, the test molecules were captured by antibodies that bind specifically to the protein and detected by anti-human IgG-F(ab)' conjugated to HRP following the procedures described above.

BV ELISA

The BV ELISA measures nonspecific binding to BV particles as an indicator of general nonspecific binding properties of mAbs.⁷ A 25 µL suspension of 1% BV particles prepared in coating buffer (0.05 sodium carbonate, pH 9.6) was added to individual wells in a 384-well plate (Cat# 464718, Nunc-Immuno Plate MaxiSorp Surface, Thermo Fisher Scientific) and incubated overnight at 4°C. Wells were blocked with 50 µL of assay buffer (PBS containing 5% BSA and 10 PPM Proclin) for 1 h at room temperature with gentle shaking. After washing the wells three times with 100 µL washing buffer (PBS), 25 µL samples prepared in assay buffer were

loaded in duplicate and incubated for 1 h at room temperature with gentle shaking. Plates were washed six times with 100 μ L washing buffer before 25 μ L of goat anti-human Fc γ fragment specific conjugated to HRP (Jackson ImmunoResearch Laboratories) at 10 ng/mL in the assay buffer was added to each well and incubated for 1 h at room temperature with gentle shaking. After washing six times with 100 μ L washing buffer, a 25 μ L aliquot of TMB (Kirkegaard & Perry Laboratories) substrate was added per well for 15 min at room temperature with gentle shaking. The reactions were stopped by adding 25 μ L of 1 M phosphoric acid. The absorbance at 450 nm was measured using a plate reader.

FcRn binding affinity measurement

The Octet RED96 system (ForteBio, Fremont, CA, USA) was used for *in vitro* FcRn-binding assays at 30°C in 96-well solid black plates (Cat# 655900, Greiner Bio-One, Monroe, NC, USA). FcRn was immobilized to nickel-nitrilotriacetic acid-coated biosensors (Cat# 18-0029, ForteBio) for 180 s at an optimized concentration. After adjusting the baseline, the mAb-FcRn binding rate was determined when the biosensor with immobilized FcRn was exposed to the mAb sample for 30 s in PBS that was adjusted to pH 6.0 with HCl. Prior to analysis, antibodies were dialyzed in PBS pH 6.0, diluted to 100 mg/mL in PBS pH 6.0 and used at a 200 μ L volume. Each assay on a specific mAb was performed in quintuplicate. Data analysis was performed using software version 7.0 (ForteBio).

pI determination by imaged capillary isoelectric focusing

Imaged capillary isoelectric focusing was performed on an iCE280 Analyzer (ProteinSimple, Toronto, Canada) as described previously.⁵⁹ The anolyte and catholyte were 80 mM phosphoric acid and 100 mM NaOH, respectively, each prepared with 0.1% methylcellulose. The mAb samples were prepared in water containing carboxypeptidase and incubated at 37°C for 20 min to remove C-terminal lysine residues. The ampholyte mixture was combined with the carboxypeptidase-treated antibodies at a final concentration of 0.25 mg/mL. Electropherograms were imaged with the optical absorption detector at 280 nm.

Cell binding assay by flow cytometry

The cells were stained with test molecules at 100 μ g/mL in FACS buffer (PBS 1% BSA, 2 mM EDTA, 0.1% sodium azide) and incubated for 1 h on ice. After washing with FACS buffer, cells were stained with PE-conjugated mouse anti-human IgG Fc secondary antibody (Cat# 9040-09, Southern Biotech, Birmingham, AL, USA) for 1 h on ice. Cells were washed and fix with fixation buffer (Cat# 554655, BD Biosciences, San Jose, CA, USA). The fluorescence intensity of stained cells was measured using a FACSCanto II flow cytometer (BD Biosciences) and the data were analyzed using FlowJo software (Tree Star, Ashland, OR, USA).

Mouse PK study with X-Fc sialylation variants

A single intravenous bolus dose of each X-Fc sialylation variant was administered to CD1 mice at 1 mg/kg dose. At various timepoints up to 21 d post-dose, serum samples ($n = 4$ /timepoint) were collected and analyzed for drug concentrations. Drug concentrations in serum were measured using a validated ELISA. Serum concentration-time data from individual animals were used to estimate PK parameters by a non-compartmental sparse analysis using Phoenix WinNonlin, version 6.4.0.768 (WinNonlin 6.4; Pharsight Corporation, Mountain View, CA, USA).

Total antibody concentrations in mouse serum were measured with an ELISA using the Gyros technology platform (Gyros US Inc., Warren, NJ, USA) and a generic PK assay as described by Williams *et al.*⁶⁰ This assay uses biotinylated sheep anti-human IgG antibody as the capture antibody and Alexa Fluor 647-conjugated sheep anti-human IgG as the detection antibody. The minimum dilution for this assay was 1:10. The assay has a standard curve range of 0.03--30 μ g/mL for mouse serum.

Acknowledgments

The authors would like to thank Patricia Y. Siguenza for her support of the project; Drs Lynn Kamen, Sivan Cohen, Gabriele Schaefer, Gail Phillips, and Noel Dybdal for providing valuable comments on the manuscript; and colleagues at the Department of Protein Analytical Chemistry, the Core Biophysical Characterization and Reagent Facility, and the Critical Reagents System for providing critical reagents.

Disclosure of Potential Conflicts of Interest

All authors are current or former employees of Genentech, Inc., a member of the Roche Group, which supported the study financially.

Funding

This work was funded and conducted by Genentech, Inc.

Abbreviations

mAb	Monoclonal antibody
FcRn	Neonatal Fc receptor
MHC	Major histocompatibility complex
B2M	β 2 microglobulin
TEER	Trans-epithelial electrical resistance
MDCK	Madin-Darby Canine Kidney
FACS	Florescence-activated cell sorting

ORCID

Shan Chung  <http://orcid.org/0000-0002-5494-2103>
 Yuwen Linda Lin  <http://orcid.org/0000-0001-8390-6964>
 Julien Lafrance-Vanasse  <http://orcid.org/0000-0001-8807-6277>
 Suzie J. Scales  <http://orcid.org/0000-0003-2544-0283>
 An Song  <http://orcid.org/0000-0001-7446-4359>

References

- Deng R, Loyet KM, Lien S, Iyer S, DeForge LE, Theil F-P, Lowman HB, Fielder PJ, Prabhu S. Pharmacokinetics of

- humanized monoclonal anti-tumor necrosis factor- α antibody and its neonatal Fc receptor variants in mice and cynomolgus monkeys. *Drug Metab Dispos.* 2010;38:600–05. doi:10.1124/dmd.109.031310. PMID:20071453.
2. Kamath AV. Translational pharmacokinetics and pharmacodynamics of monoclonal antibodies. *Drug Discov Today Technol.* 2016;21–22:75–83. doi:10.1016/j.ddtec.2016.09.004.
 3. Igawa T, Tsunoda H, Tachibana T, Maeda A, Mimoto F, Moriyama C, Nanami M, Sekimori Y, Nabuchi Y, Aso Y, et al. Reduced elimination of IgG antibodies by engineering the variable region. *Protein Eng Des Sel.* 2010;23:385–92. doi:10.1093/protein/gzq009. PMID:20159773.
 4. Bumbaca Yadav D, Sharma VK, Boswell CA, Hotzel I, Tesar D, Shang Y, Ying Y, Fischer SK, Grogan JL, Chiang EY, et al. Evaluating the use of antibody variable region (Fv) charge as a risk assessment tool for predicting typical cynomolgus monkey pharmacokinetics. *J Biol Chem.* 2015;290:29732–41. doi:10.1074/jbc.M115.692434. PMID:26491012.
 5. Datta-Mannan A, Thangaraju A, Leung D, Tang Y, Witcher DR, Lu J, Wroblewski VJ. Balancing charge in the complementarity-determining regions of humanized mAbs without affecting pI reduces non-specific binding and improves the pharmacokinetics. *MAbs.* 2015;7:483–93. doi:10.1080/19420862.2015.1016696. PMID:25695748.
 6. Sharma VK, Patapoff TW, Kabakoff B, Pai S, Hilario E, Zhang B, Li C, Borisov O, Kelley RF, Chorny I, et al. In silico selection of therapeutic antibodies for development: viscosity, clearance, and chemical stability. *Proc Natl Acad Sci U S A.* 2014;111:18601–06. doi:10.1073/pnas.1421779112. PMID:25512516.
 7. Hotzel I, Theil FP, Bernstein LJ, Prabhu S, Deng R, Quintana L, Lutman J, Sibia R, Chan P, Bumbaca D, et al. A strategy for risk mitigation of antibodies with fast clearance. *MAbs.* 2012;4:753–60. doi:10.4161/mabs.22189. PMID:23778268.
 8. Bumbaca D, Wong A, Drake E, Reyes AE 2nd, Lin BC, Stephan J-P, Desnoyers L, Shen B-Q, Dennis MS. Highly specific off-target binding identified and eliminated during the humanization of an antibody against FGF receptor 4. *MAbs.* 2011;3:376–86. PMID:21540647.
 9. Stefanich EG, Ren S, Danilenko DM, Lim A, Song A, Iyer S, Fielder PJ. Evidence for an asialoglycoprotein receptor on non-parenchymal cells for O-linked glycoproteins. *J Pharmacol Exp Ther.* 2008;327:308–15. doi:10.1124/jpet.108.142232. PMID:18728239.
 10. Yu M, Brown D, Reed C, Chung S, Lutman J, Stefanich E, Wong A, Stephan J-P, Bayer R. Production, characterization, and pharmacokinetic properties of antibodies with N-linked mannose-5 glycans. *MAbs.* 2012;4:475–87. doi:10.4161/mabs.20737. PMID:22699308.
 11. Mortensen DL, Prabhu S, Stefanich EG, Kadkhodayan-Fischer S, Gelzleichter TR, Baker D, Jiang J, Wallace K, Iyer S, Fielder PJ, et al. Effect of antigen binding affinity and effector function on the pharmacokinetics and pharmacodynamics of anti-IgE monoclonal antibodies. *MAbs.* 2012;4:724–31. doi:10.4161/mabs.22216. PMID:23778267.
 12. Chirmule N, Jawa V, Meibohm B. Immunogenicity to therapeutic proteins: impact on PK/PD and efficacy. *Aaps J.* 2012;14:296–302. doi:10.1208/s12248-012-9340-y. PMID:22407289.
 13. Dall'Acqua WF, Kiener PA, Wu H. Properties of human IgG1s engineered for enhanced binding to the neonatal Fc receptor (FcRn). *J Biol Chem.* 2006;281:23514–24. doi:10.1074/jbc.M604292200. PMID:16793771.
 14. Suzuki T, Ishii-Watabe A, Tada M, Kobayashi T, Kanayasu-Toyoda T, Kawanishi T, Yamaguchi T. Importance of neonatal FcR in regulating the serum half-life of therapeutic proteins containing the Fc domain of human IgG1: a comparative study of the affinity of monoclonal antibodies and Fc-fusion proteins to human neonatal FcR. *J Immunol.* 2010;184:1968–76. doi:10.4049/jimmunol.0903296. PMID:20083659.
 15. Gurbaxani B, Dostalek M, Gardner I. Are endosomal trafficking parameters better targets for improving mAb pharmacokinetics than FcRn binding affinity? *Mol Immunol.* 2013;56(4):660–74. doi:10.1016/j.molimm.2013.05.008.
 16. Pyzik M, Rath T, Lencer WI, Baker K, Blumberg RS. FcRn: the architect behind the immune and nonimmune functions of IgG and albumin. *J Immunol.* 2015;194:4595–603. doi:10.4049/jimmunol.1403014. PMID:25934922.
 17. Ward ES, Devanaboyina SC, Ober RJ. Targeting FcRn for the modulation of antibody dynamics. *Mol Immunol.* 2015;67:131–41. doi:10.1016/j.molimm.2015.02.007. PMID:25766596.
 18. Ghetie V, Ward ES. Transcytosis and catabolism of antibody. *Immunol Res.* 2002;25:97–113. doi:10.1385/IR.25:2:097.
 19. Dickinson BL, Badizadegan K, Wu Z, Ahouse JC, Zhu X, Simister NE, Blumberg RS, Lencer WI. Bidirectional FcRn-dependent IgG transport in a polarized human intestinal epithelial cell line. *J Clin Invest.* 1999;104(7):903–11. doi:10.1172/JCI6968.
 20. Tzaban S, Massol RH, Yen E, Hamman W, Frank SR, Lapierre LA, Hansen SH, Goldenring JR, Blumberg RS, Lencer WI. The recycling and transcytotic pathways for IgG transport by FcRn are distinct and display an inherent polarity. *J Cell Biol.* 2009;185(4):673–84. doi:10.1083/jcb.200809122.
 21. Avery LB, Wang M, Kavosi MS, Joyce A, Kurz JC, Fan -Y-Y, Dowty ME, Zhang M, Zhang Y, Cheng A, et al. Utility of a human FcRn transgenic mouse model in drug discovery for early assessment and prediction of human pharmacokinetics of monoclonal antibodies. *MAbs.* 2016;8:1064–78. doi:10.1080/19420862.2016.1193660. PMID:27232760.
 22. Vugmeyer Y, Xu X, Theil F-P, Khawli LA, Leach MW. Pharmacokinetics and toxicology of therapeutic proteins: advances and challenges. *World J Biol Chem.* 2012;3:73–92. doi:10.4331/wjbc.v3.i4.73. PMID:22558487.
 23. Deng R, Iyer S, Theil F-P, Mortensen DL, Fielder PJ, Prabhu S. Projecting human pharmacokinetics of therapeutic antibodies from nonclinical data: what have we learned? *MAbs.* 2011;3:61–66. PMID:20962582.
 24. Wang J, Iyer S, Fielder PJ, Davis JD, Deng R. Projecting human pharmacokinetics of monoclonal antibodies from nonclinical data: comparative evaluation of prediction approaches in early drug development. *Biopharm Drug Dispos.* 2016;37:51–65. doi:10.1002/bdd.1952. PMID:25869767.
 25. Sampei Z, Igawa T, Soeda T, Okuyama-Nishida Y, Moriyama C, Wakabayashi T, Tanaka E, Muto A, Kojima T, Kitazawa T, et al. Identification and multidimensional optimization of an asymmetric bispecific IgG antibody mimicking the function of factor VIII cofactor activity. *PLoS One.* 2013;8(2):e57479. PMID:23468998. doi:10.1371/journal.pone.0057479.
 26. Schlothauer T, Rueger P, Stracke JO, Hertenberger H, Fingas F, Kling L, Emrich T, Drabner G, Seeber S, Auer J, et al. Analytical FcRn affinity chromatography for functional characterization of monoclonal antibodies. *MAbs.* 2013;5:576–86. doi:10.4161/mabs.24981. PMID:23765230.
 27. Souders CA, Nelson SC, Wang Y, Crowley AR, Klempner MS, Thomas W Jr. A novel in vitro assay to predict neonatal Fc receptor-mediated human IgG half-life. *MAbs.* 2015;7:912–21. doi:10.1080/19420862.2015.1054585. PMID:26018774.
 28. Praetor A, Ellinger I, Hunziker W. Intracellular traffic of the MHC class I-like IgG Fc receptor, FcRn, expressed in epithelial MDCK cells. *J Cell Sci.* 1999;112:2291–99.
 29. Claypool SM, Dickinson BL, Yoshida M, Lencer WI, Blumberg RS. Functional reconstitution of human FcRn in Madin-Darby canine kidney cells requires co-expressed human beta 2-microglobulin. *J Biol Chem.* 2002;277:28038–50. doi:10.1074/jbc.M202367200.
 30. Tesar DB, Tiangco NE, Bjorkman PJ. Ligand valency affects transcytosis, recycling and intracellular trafficking mediated by the neonatal Fc receptor. *Traffic.* 2006;7:1127–42. PMID:17004319.
 31. Sockolovsky JT, Tiffany MR, Szoka FC. Engineering neonatal Fc receptor-mediated recycling and transcytosis in recombinant

- proteins by short terminal peptide extensions. *Proc Natl Acad Sci U S A*. 2012;109(40):16095–100. doi:10.1073/pnas.1208857109.
32. Ying T, Wang Y, Feng Y, Prabakaran P, Gong R, Wang L, Crowder K, Dimitrov DS. Engineered antibody domains with significantly increased transcytosis and half-life in macaques mediated by FcRn. *MAbs*. 2015;7(5):922–30. doi:10.1080/19420862.2015.1067353.
 33. Jaramillo CAC, Belli S, Cascais A-C, Dudal S, Edelman MR, Haak M, Brun M-E, Otteneder MB, Ullah M, Funk C, et al. Toward in vitro-to-in vivo translation of monoclonal antibody pharmacokinetics: application of a neonatal Fc receptor-mediated transcytosis assay to understand the interplaying clearance mechanisms. *MAbs*. 2017;9:781–91. doi:10.1080/19420862.2017.1320008.
 34. Chung S, Lin YL, Nguyen V, Kamen L, Zheng K, Vora B, Song A. Development of a label-free FcRn-mediated transcytosis assay for in vitro characterization of FcRn interactions with therapeutic antibodies and Fc-fusion proteins. *J Immunol Methods*. 2018. doi:10.1016/j.jim.2018.07.004. PMID:30030147.
 35. Grevys A, Nilsen J, Sand KMK, Daba MB, Øynebråten I, Bern M, McAdam MB, Foss S, Schlothauer T, Michaelsen TE, et al. A human endothelial cell-based recycling assay for screening of FcRn targeted molecules. *Nat Commun*. 2018;9(1):621. doi:10.1038/s41467-018-03061-x.
 36. Goebel NA, Babbey CM, Datta-Mannan A, Witcher DR, Wroblewski VJ, Dunn KW, Schmid SL. Neonatal Fc receptor mediates internalization of Fc in transfected human endothelial cells. *Mol Biol Cell*. 2008;9:5490–505. doi:10.1091/mbc.e07-02-0101.
 37. Chaudhury C, Mehnaz S, Robinson JM, Hayton WL, Pearl DK, Roodenian DC, Anderson CL. The major histocompatibility complex-related Fc receptor for IgG (FcRn) binds albumin and prolongs its lifespan. *J Exp Med*. 2003;197:315–22. PMID:12566415.
 38. Quartino AL, Hillenbach C, Li J, Li H, Wada RD, Visich J, Li C, Heinzmann D, Jin JY, Lum BL. Population pharmacokinetic and exposure-response analysis for trastuzumab administered using a subcutaneous “manual syringe” injection or intravenously in women with HER2-positive early breast cancer. *Cancer Chemother Pharmacol*. 2016;77:77–88. doi:10.1007/s00280-015-2922-5. PMID:26645407.
 39. Quartino AL, Li H, Jin JY, Wada DR, Benyunes MC, McNally V, Viganò L, Nijem I, Lum BL, Garg A. Pharmacokinetic and exposure-response analyses of pertuzumab in combination with trastuzumab and docetaxel during neoadjuvant treatment of HER2+ early breast cancer. *Cancer Chemother Pharmacol*. 2017;79:353–61. doi:10.1007/s00280-016-3218-0. PMID:28074265.
 40. Ng CM, Joshi A, Dedrick RL, Garovoy MR, Bauer RJ. Pharmacokinetic-pharmacodynamic-efficacy analysis of efalizumab in patients with moderate to severe psoriasis. *Pharm Res*. 2005;22:1088–100. doi:10.1007/s11095-005-5642-4. PMID:16028009.
 41. Klotz U, Teml A, Schwab M. Clinical pharmacokinetics and use of infliximab. *Clin Pharmacokinet*. 2007;46:645–60. doi:10.2165/00003088-200746080-00002. PMID:17655372.
 42. Singer J, Weichselbaumer M, Stockner T, Mechtcheriakova D, Sobanov Y, Bajna E, Wrba F, Horvat R, Thalhammer JG, Willmann M, et al. Comparative oncology: erbB-1 and ErbB-2 homologues in canine cancer are susceptible to cetuximab and trastuzumab targeting. *Mol Immunol*. 2012;50(4):200–09. doi:10.1016/j.molimm.2012.01.002.
 43. Franklin MC, Carey KD, Vajdos FF, Leahy DJ, de Vos AM, Sliwkowski MX. Insights into ErbB signaling from the structure of the ErbB2-pertuzumab complex. *Cancer Cell*. 2004;5:317–28.
 44. Cho HS, Mason K, Ramyar KX, Stanley AM, Gabelli SB, Denney DW, Leahy DJ. Structure of the extracellular region of HER2 alone and in complex with the Herceptin Fab. *Nature*. 2003;421(6924):756–60. doi:10.1038/nature01392.
 45. Boswell CA, Tesar DB, Mukhyala K, Theil FP, Fielder PJ, Khawli LA. Effects of charge on antibody tissue distribution and pharmacokinetics. *Bioconjug Chem*. 2010;21:2153–63. doi:10.1021/bc100261d. PMID:21053952.
 46. Higel F, Seidl A, Sorgel F, Friess W. N-glycosylation heterogeneity and the influence on structure, function and pharmacokinetics of monoclonal antibodies and Fc fusion proteins. *Eur J Pharm Biopharm*. 2016;100:94–100. doi:10.1016/j.ejpb.2016.01.005. PMID:26775146.
 47. Leabman MK, Meng YG, Kelley RF, DeForge LE, Cowan KJ, Iyer S. Effects of altered Fcγ₁ binding on antibody pharmacokinetics in cynomolgus monkeys. *MAbs*. 2013;5:896–903. doi:10.4161/mabs.26436. PMID:24492343.
 48. Lee SJ, Evers S, Roeder D, Parlow AF, Risteli J, Risteli L, Lee YC, Feizi T, Langen H, Nussenzweig MC. Mannose receptor-mediated regulation of serum glycoprotein homeostasis. *Science*. 2002;295:1898–901. doi:10.1126/science.1069540. PMID:11884756.
 49. Stockert RJ. The asialoglycoprotein receptor: relationships between structure, function, and expression. *Physiol Rev*. 1995;75:591–609. doi:10.1152/physrev.1995.75.3.591. PMID:7624395.
 50. Kenanova V, Olafsen T, Crow DM, Sundaresan G, Subbarayan M, Carter NH, Ikke DN, Yazaki PJ, Chatziioannou AF, Gambhir SS, et al. Tailoring the pharmacokinetics and positron emission tomography imaging properties of anti-carcinoembryonic antigen single-chain Fv-Fc antibody fragments. *Cancer Res*. 2005;65:622–31. PMID:15695407.
 51. Wang W, Lu P, Fang Y, Hamuro L, Pittman T, Carr B, Hochman J, Prueksaritanont T. Monoclonal antibodies with identical Fc sequences can bind to FcRn differentially with pharmacokinetic consequences. *Drug Metab Dispos*. 2011;39:1469–77. doi:10.1124/dmd.111.039453.
 52. Hu J, Liu J, Yang D, Lu M, Yin J. Physiological roles of asialoglycoprotein receptors (ASGPRs) variants and recent advances in hepatic-targeted delivery of therapeutic molecules via ASGPRs. *Protein Pept Lett*. 2014;21:1025–30.
 53. Wright A, Sato Y, Okada T, Chang K, Endo T, Morrison S. In vivo trafficking and catabolism of IgG1 antibodies with Fc associated carbohydrates of differing structure. *Glycobiology*. 2000;10:1347–55.
 54. Cianga P, Medesan C, Richardson JA, Ghetie V, Ward ES. Identification and function of neonatal Fc receptor in mammary gland of lactating mice. *Eur J Immunol*. 1999;29:2515–23. doi:10.1002/(SICI)1521-4141(199908)29:08<2515::AID-IMMU2515>3.0.CO;2-D. PMID:10458766.
 55. Antohe F, Radulescu L, Gafencu A, Ghetie V, Simionescu M. Expression of functionally active FcRn and the differentiated bidirectional transport of IgG in human placental endothelial cells. *Hum Immunol*. 2001;62:93–105. PMID:11182218.
 56. Sarav M, Wang Y, Hack BK, Chang A, Jensen M, Bao L, Quigg RJ. Renal FcRn reclaims albumin but facilitates elimination of IgG. *J Am Soc Nephrol*. 2009;20:1941–52. doi:10.1681/ASN.2008090976. PMID:19661163.
 57. Yip V, Palma E, Tesar DB, Mundo EE, Bumbaca D, Torres EK, Reyes NA, Shen BQ, Fielder PJ, Prabhu S, et al. Quantitative cumulative biodistribution of antibodies in mice: effect of modulating binding affinity to the neonatal Fc receptor. *MAbs*. 2014;6:689–96. doi:10.4161/mabs.28254. PMID:24572100.
 58. Kim JH, Lee SR, Li LH, Park HJ, Park JH, Lee KY, Kim M-K, Shin BA, Choi S-Y, Thiel V. High cleavage efficiency of a 2A peptide derived from porcine teschovirus-1 in human cell lines, zebrafish and mice. *PLoS One*. 2011;6:e18556. doi:10.1371/journal.pone.0018556. PMID:21602908.
 59. Li B, Tesar D, Boswell CA, Cahaya HS, Wong A, Zhang J, Meng YG, Eigenbrot C, Pantua H, Diao J, et al. Framework selection can influence pharmacokinetics of a humanized therapeutic antibody through differences in molecule charge. *MAbs*. 2014;6:1255–64. doi:10.4161/mabs.29809. PMID:25517310.
 60. Williams K, Erickson R, Fischer SK. Overcoming disease-specific matrix effect in a clinical pharmacokinetic assay using a microfluidic immunoassay technology. *Bioanalysis*. 2017;9:1207–16. doi:10.4155/bio-2017-0102. PMID:28766364.